Available online at www.sciencedirect.com
ScienceDirect
International Journal of Pharmaceutics 346 (2008) 160–168
INTERNATIONAL JOURNAL OF PHARMACEUTICS
www.elsevier.com/locate/ijpharm

Pharmaceutical Nanotechnology

Preparation, physicochemical characterization, and antioxidant effects of quercetin nanoparticles

Tzu-Hui Wu [a,b], Feng-Lin Yen [a], Liang-Tzung Lin [c], Tong-Rong Tsai [d], Chun-Ching Lin [d,*], Thau-Ming Cham [d,**]

[a] *Graduate Institute of Pharmaceutical Science, College of Pharmacy, Kaohsiung Medical University, Kaohsiung, Taiwan*
[b] *Health Bureau of Kaohsiung County Government, Kaohsiung, Taiwan*
[c] *Department of Microbiology and Immunology, Dalhousie University, Halifax, Nova Scotia, Canada*
[d] *Faculty of Pharmacy, College of Pharmacy, Kaohsiung Medical University, Kaohsiung, Taiwan*

Received 5 February 2007; received in revised form 24 April 2007; accepted 13 June 2007
Available online 28 June 2007

Abstract

The purpose of this study was to develop quercetin-loaded nanoparticles (QUEN) by a nanoprecipitation technique with Eudragit® E (EE) and polyvinyl alcohol (PVA) as carriers, and to evaluate the antioxidant effects of quercetin (QU) and of its nanoparticles. The novel QUEN systems were characterized by particle size and morphology, yield and encapsulation efficiency, differential scanning calorimetry (DSC), powder X-ray diffraction (XRD), Fourier transform infrared spectroscopy (FT-IR), ^{1}H nuclear magnetic resonance (^{1}H NMR), and dissolution study. It was observed that the weight ratio of QU:EE:PVA at 1:10:10 carried a particle size of <85 nm, a particle distribution with polydispersity index <0.3, and its yield and encapsulation efficiency were over 99%. The results from XRD and DSC of the QUEN showed that the crystal of the drug might be converted to an amorphous state. The FT-IR and ^{1}H NMR demonstrated that QU formed intermolecular hydrogen bonding with carriers. The release of the drug from the QUEN was 74-fold higher compared with the pure drug. In addition, the antioxidant activity of the QUEN was more effective than pure QU on DPPH scavenging, anti-superoxide formation, superoxide anion scavenging, and anti-lipid peroxidation.

Keywords: Quercetin; Nanoparticles; ^{1}H nuclear magnetic resonance; Free radical-scavenging activity; Anti-lipid peroxidation

1. Introduction

Reactive oxygen species (ROS), such as superoxide anion, hydroxyl radical, and hydrogen peroxide, have a causal relationship with oxidative stress. Many studies have demonstrated that overproduction of ROS can further aggravate the oxidative stress and the result is a unifying mechanism of injury in many developments of clinical disease processes, such as heart disease (Giordano, 2005), diabetes (Rolo and Palmeira, 2006), liver injury (Jaeschke, 2000), cancer (Klaunig and Kamendulis, 2004), aging (Bokov et al., 2004), etc. The balance of ROS and antioxidant is a major mechanism in preventing damage by oxidative stress. Therefore, the dietary supplement of antioxidants such as vitamins (Fairfield and Fletcher, 2002), flavonoids (Peluso, 2006), etc., has been used to prevent the occurrence of many chronic diseases.

Quercetin (QU) (Fig. 1), is a well-known flavonoid distributed ubiquitously in fruits, vegetables, and herbs or related products, e.g. apples, onions (Hertog et al., 1992), *Ginkgo biloba* (Watson and Oliveira, 1999), and red wine (Kerem et al., 2004), respectively. QU has been extensively investigated for its pharmacological effects that include anti-tumor (Kanadaswami et al., 2005), anti-inflammatory (Comalada et al., 2005), antioxidant (Inal and Kahraman, 2000), and hepatoprotective (Lee et al., 2003) activities.

Clinical studies investigating different programs of administration of QU have been limited by its poor water solubility. Many researchers have attempted to improve its solubility by adding dimethylsulfoxide (DMSO) (Ader et al., 2000). How-

* Corresponding author at: Faculty of Pharmacy, College of Pharmacy, Kaohsiung Medical University, 100 Shih-Chuan 1st Road, Kaohsiung 807, Taiwan. Tel.: +886 7 3121101x2122; fax: +886 7 3135215.
** Corresponding author at: Faculty of Pharmacy, College of Pharmacy, Kaohsiung Medical University, 100, Shih-Chuan 1st Road, Kaohsiung 807, Taiwan. Tel.: +886 7 3121101x2254; fax: +886 7 3210683.
E-mail addresses: aalin@kmu.edu.tw (C.-C. Lin), chamtm@kmu.edu.tw (T.-M. Cham).

0378-5173/$ – see front matter © 2007 Elsevier B.V. All rights reserved.
doi:10.1016/j.ijpharm.2007.06.036

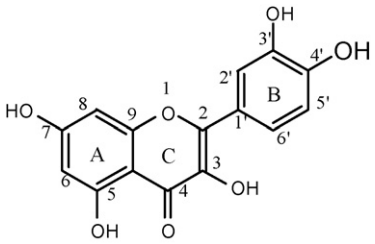

Fig. 1. Chemical structure of quercetin (3,3′,4′,5,7-pentahydroxylflavone).

ever, the safety of the higher DMSO is questionable due to risk of vasoconstrictor effect and neurological toxicity (Windrum et al., 2005). Additionally, a water-soluble derivative of QU has been synthesized but its bioavailability was only 20% (Mulholland et al., 2001). Various techniques have also been used to increase the solubility of QU including the complexation with cyclodextrin and liposome (Pralhad and Rajendrakumar, 2004; Yuan et al., 2006). Nevertheless, the use of cyclodextrin is associated with a risk of nephrotoxicity (Frijlink et al., 1991) and employing liposome might incur stability problems during storage (Mu and Zhong, 2006). It is therefore clear that a safe, stable, and efficient delivery method in increasing the solubility of QU is warranted.

Nanoparticles are particularly useful in drug delivery for water-insoluble compounds such as cyclosporine A (Dai et al., 2004), ellagic acid (Bala et al., 2006) and coenzymeQ10 (Hsu et al., 2003) because their size (less than 1000 nm) can increase the absorption and the bioavailability of the delivered drug. A novel quercetin nanoparticles system (QUEN) was therefore prepared by a simple nanoprecipitation technology with Eudragit® E (EE) and polyvinyl alcohol (PVA) as carriers. The physicochemical characterization of the QUEN was inspected by transmission electron microscopy (TEM), differential scanning calorimetry (DSC), powder X-ray diffraction (XRD), Fourier transform infrared spectroscopy (FT-IR), ^{1}H nuclear magnetic resonance (^{1}H NMR), and dissolution study. Furthermore, the antioxidant effects of pure QU and of its nanoparticles were also determined by free radical scavenging, anti-lipid peroxidation, anti-superoxide formation, and scavenging superoxide studies.

2. Materials and methods

2.1. Materials

Quercetin (QU), polyvinyl alcohol (PVA), Tris–HCl, thiobarbituric acid (TBA), ferrous chloride, ascorbate, xanthine, xanthine oxidase, cytochrome *c*, 2,2-diphenyl-1-picrylhydrazyl (DPPH), dimethyl sulfoxide (DMSO), and ethylenediaminetetraacetic acid (EDTA) were purchased from Sigma–Aldrich Chemicals Co. (St. Louis, MO, USA). Aminoalkyl methacrylate copolymers (Eudragit® E; EE) were obtained from Röhm Pharma (Dramstadt, Germany). All other chemical regents were of analytical grade.

2.2. HPLC analysis of quercetin

The chromatographic system was composed of a pump P-680, autosampler ASI-100, and UVD-170U detector. The analytical column used was the LichroCART® Purospher® STAR (250 mm × 4.6 mm i.d., 5 μm) and the temperature must be maintained at 37 °C. The mobile phase was composed of 25 mM phosphate buffer and acetonitrile (50:50), and pH value was adjusted to 2.3 with hydrochloride acid. The flow rate was set at 0.5 ml/min. The wavelength of UV detector was kept at 258 nm. The calibration curve of quercetin was linear ($r = 0.9999$) within range 1–100 μg/ml. The relative standard deviations of the intra-day and interday were less than 5% ($n = 5$).

2.3. Preparations of physical mixtures and nanoparticles systems

2.3.1. Physical mixtures

The physical mixtures were pulverized and mixed with different ratios of QU:EE:PVA (1:1:1, 1:5:5, and 1:10:10; w/w/w) in a mortar.

2.3.2. Nanoparticles systems

Nanoparticles systems were prepared with various ratios of QU:EE:PVA (1:1:1, 1:5:5, and 1:10:10; w/w/w) by the nanoprecipitation technique (Bilati et al., 2005; Zili et al., 2005). An amount of 100 mg of quercetin and the appropriate amount of EE were dissolved in 50 ml of ethanol. The internal organic phase solutions were quickly injected into the 150 ml external aqueous solution containing the appropriate amount of PVA, and then the solutions were homogenized at 22,000 rpm for 25 min. The ethanol was completely removed by rotary vacuum evaporation at 40 °C water bath and then lyophilized with a freeze dryer. The lyophilized powders were collected and stored in the moisture-proof instrument until use.

2.4. Particle size analysis

The mean particle size and polydispersity index (PI) of the QUEN were determined by a N5 submicron particles size analyzer (Beckman Coulter, USA). The samples were diluted 10-times with distilled water for analysis. Each value was measured in triplicate determination. The results are showed as mean ± standard distribution.

2.5. Yield and encapsulation efficiency

Regarding the yield of the QUEN, the appropriate volume of each sample was dissolved in methanol and the drug concentration was measured by the above-mentioned HPLC method. Additionally, the encapsulation efficiency of the QUEN was conducted according to the modified procedures described previously (Venkateswarlu and Manjunath, 2004). The encapsulated and unencapsulated portions of QU from the QUEN were separated using the centrifugal filter devices (Microcon YM-10, Millipore®) with centrifuged at 10,000 rpm for 30 min. The yield and encapsulation efficiency of QU can be calculated by the following equations (1) and (2):

$$\text{yield } (\%) = C_Q \times \frac{V_Q}{W_Q} \times 100 \quad (1)$$

$$\text{encapsulation efficiency } (\%) = \frac{(C_Q V_Q) - (F_Q V_Q)}{C_Q V_Q} \times 100 \quad (2)$$

where C_Q was the concentration of QU from the QUEN; W_Q was the theoretical amount of QU added; V_Q was the volume of QU from the QUEN; F_Q was the concentration of QU in unencapsulated portion.

2.6. Partition coefficient analysis

The logarithm of partition coefficients of QU and EE in *n*-octanol/water (1:1) was conducted according to the modified method as described by Liao and Yin (2000). A concentration of 100 μg of QU and 750 μg of EE were added to 10 ml *n*-octanol/water (phosphate buffer, pH 7.4) (1:1) and then mixed 1 min by vortex, respectively. The concentrations of QU and EE in octanol layer were determined by UV spectrometer (Hitachi U-2001). The log K_{oct}/water value can be calculated by the following formula: (its concentration in *n*-octanol/its concentration in water). A partition coefficient value > 1 indicated a more hydrophobic property.

2.7. Transmission electron microscopy (TEM)

The morphology of the QUEN was examined by a transmission electron microscope (JEOL JEM-2000 EXII TEM, Tokyo, Japan). Before analyzing, the samples were stained with 0.5% (w/v) phosphotungstic acid and fixed on copper grids for observation.

2.8. Differential scanning calorimetry (DSC)

The thermograms of pure materials and lyophilized QUEN were determined using a differential scanning calorimetry (DSC-7, Perkin-Elmer, Norwalk, CT). Approximately 3 mg of each sample was heated in aluminum pans from 50–350 °C and the scanning rate was conducted at 10 °C min^{-1}.

2.9. X-ray diffractometry (XRD)

The patterns of pure materials, their physical mixtures, and lyophilized QUEN were obtained using the X-ray diffractometer (Siemens D5000, Germany) with Ni-filtered Cu Kα radiation. Measurements were performed at a voltage of 40 kV and 25 mA. The scanned angle was set from $2^\circ \leq 2\theta \geq 50^\circ$, and the scanned rate was 1° min^{-1}. Measurements were made in triplicate.

2.10. Fourier transform infrared (FT-IR) spectroscopy

The FT-IR spectra of the samples were obtained on a Perkin-Elmer 2000 spectrophotometer (Perkin-Elmer, Norwalk, CT, USA). Each sample and potassium bromide were mixed by an agate mortar and compressed into thin tablets. The scanning range was 370–4000 cm^{-1} and the resolution was 1 cm^{-1}. Each sample was measured and recorded in triplicate.

2.11. ^1H nuclear magnetic resonance (^1H NMR) spectroscopy

The ^1H NMR spectra of QU and QUEN were recorded using a JEOL Alpha 400 spectrometer (Nihon Denshi Co., Tokyo, Japan). An amount of 50 mg of each sample was dissolved in 0.8 ml of DMSO-d_6 and each sample was measured and recorded in triplicate.

2.12. Dissolution study

Dissolution studies of QU, its physical mixtures, and of the QUEN were performed in the simulated gastric fluid (USP XXIV). Samples equivalent to 5 mg of QU were placed in the 100 ml simulated gastric fluid which was stirred with rotating paddle at 100 rpm. Then, 0.5 ml of each sample was withdrawn at time intervals of 5, 10, 20, 40, 60, 90 and 120 min, and filtrated by a 0.02 μm filter (Anodisc 25, Whatman®). The concentrations of drug were determined by HPLC analysis as mentioned above.

2.13. Antioxidant activities assays

2.13.1. DPPH scavenging

DPPH, a stable free radical, has been evaluated in many studies to determine the free radical-scavenging activity of compounds or plant extractions (Bao et al., 2005; Castro et al., 2006). A concentration of 200 μM of DPPH ethanol solution was prepared. A series of concentrations of pure QU dissolved in distilled water or DMSO and its nanoparticles dissolved in distilled water were prepared. One hundred and twenty-five microliters of different samples were mixed with 125 μl DPPH solution and incubated at room temperature. After 30 min, the absorbance of the reaction solution was measured by an ELISA reader at 517 nm. The percentage of scavenging of free radical by the sample was calculated according to the following equation: % scavenging effect = [(Ab517 control − Ab517 sample)/Ab517 control] × 100. The scavenging concentration of each sample at 50% (SC_{50}) was used to compare the free radical-scavenging activity, and all determinations were performed in triplicate.

2.13.2. Anti-superoxide formation assay

Xanthine oxidase inhibition activity was measured by the formation of uric acid (Chang et al., 1994). To assess superoxide anion formation, 50 μl of test samples solution, 400 μl of KH_2PO_4 (0.1 mM), 530 μl of de-ionized water, and 20 μl of xanthine oxidase (1 unit/ml) were added into a cuvette and then shaken for 2 min. The superoxide anion formation was then determined by spectrophotometric measurement of uric acid production at 295 nm. All determinations were performed in triplicate. The percentage of inhibition was calculated using the following equation: % inhibition = [(Ab295 control − Ab295 sample)/Ab295 control] × 100. The inhibition concentration of each sample at 50% (IC_{50}) was used to compare the anti-superoxide formation.

2.13.3. Superoxide anion-scavenging activity assay

Enzyme formation of superoxide anion was estimated by the reduction of cytochrome *c* method (McCord and Fridovich, 1969; Yu et al., 2001). First, the reagent solution was prepared by adding 50 mM of KH_2PO_4, 0.1 mM of EDTA, 0.1 mM of cytochrome *c* and 0.1 mM of xanthine. Subsequently, 50 μl of test samples, 400 μl of the reagent solution, 530 μl of distilled water, and 20 μl of xanthine oxidase were added into a cuvette. All samples were incubated for 2 min at room temperature and then determined spectrophotometrically at 550 nm. All determinations were performed in triplicate. The percentage of scavenging of superoxide radical by the sample was calculated according to the equation: % scavenging effect = [(Ab550 control − Ab550 sample)/Ab550 control] × 100. The scavenging concentration of each sample at 50% (SC_{50}) was used to compare the superoxide anion-scavenging activity.

2.13.4. Anti-lipid peroxidation assay

The anti-lipid peroxidation effect of QU and the QUEN on $FeCl_2$–ascorbic acid-induced lipid peroxidation in rat liver homogenate was performed according to the previously described method (Ohkawa et al., 1979; Wong et al., 1987). The 20% liver homogenate (w/v) was prepared with 150 mM Tris–HCl buffered saline (pH 7.2) by a polytron homogenizer and further centrifuged at 500 × *g* for 10 min. Briefly, the 50 μl homogenate was mixed with 30 μl of test sample, 10 μl of 4 mM $FeCl_2$ and 10 μl of 0.2 mM ascorbic acid. The mixture was incubated at 37 °C for 1 h in a eppendorf tube, then 100 μl of 0.1N HCl, 40 μl of 9.8% SDS, 180 μl of de-ionized water, and 400 μl of 0.6% TBA were added to each tube and vigorously shaken. The tubes were placed in 95 °C for 30 min. After cooling, tubes were added 1000 μl *n*-butanol and centrifuged at 1000 × *g* for 25 min, and the supernatants were subsequently measured with a spectrophotometer (Hitachi U-2001) at 532 nm. All determinations were performed in triplicate. The percentage of lipid peroxidation inhibition was calculated following the equation: % inhibition = [1 − (Ab532 induced − Ab532 sample)/(Ab532 induced − Ab532 control)] × 100. The inhibitory concentration of the production of 50% lipid peroxide was expressed as IC_{50} and was used to compare the anti-lipid peroxidation activity.

2.14. Statistical analysis

All data were expressed as means ± standard deviations, and analyzed with one-way analysis of variance (ANOVA). Scheffe's test was used to calculate statistical significance by SPSS software. $P < 0.05$ and 0.001 were considered statistically significant.

3. Results and discussion

3.1. Characterization of quercetin nanoparticles (QUEN)

As Table 1 shows, the mean particle size and PI of the QUEN were less than 100 nm and 0.5, respectively, except for QU:PVA:EE at 1:1:1 (472.9 ± 107.73 nm and 0.74 ± 0.01). These results indicated that the small mean size and pI value can depend on the proportion of PVA. The possible explanation was that a high proportion of PVA could provide sufficient stabilization to the nanoparticles system, and reduce their particle size and size distribution (Sahoo et al., 2002; Galindo-Rodriguez et al., 2004). The morphological property of the QUEN is also shown in Fig. 2. The QUEN prepared with the QU:PVA:EE at 1:10:10 and 1:5:5 ratios presented smaller spherical shape and uniform size distributions (Fig. 2A and B). In contrast, the QU:PVA:EE at 1:1:1 was insufficient to stabilize the nanoparticles system and would lead to mutual coalescence between particles forming a larger size (Fig. 2C).

The encapsulation efficiency of QU was 94.8 ± 1.75 to 99.9 ± 0.59% and the yields were 0.17 ± 0.01 to 99.3 ± 0.57% as obtained from different ratios of QU:PVA:EE, respectively (Table 1). As the content of EE increased, the yield and encapsulation efficiency of the drug were enhanced. The most likely reason was that the lipophilic character of QU ($\log K_{oct}$/water = 1.81 ± 0.17) and EE ($\log K_{oct}$/water = 2.07 ± 0.34) can be miscible in the internal organic phase, leading to a stronger affinity between them. Consequently, a higher ratio of EE with QU was preferentially dispersed in the internal organic phase, and a slight amount of drug was lost in the aqueous phase during the process of nanoparticles preparation (Ubrich et al., 2005). Furthermore, the encapsulation efficiencies of the drug could also be influenced by adjusting the proportion of PVA. Table 1 showed that encapsulation efficiencies of QU increased with enhancing content of PVA. This finding is consistent with the reports from Sehra and Dhake (2005) and Mu and Zhong (2006). The possible reason was that the hydrophobic portion of PVA interpenetrated into the EE chains during nanoprecipitation and remained trapped to the polymeric matrix of the nanoparticles. Accordingly, the addition of PVA easily formed an interconnected network with

Table 1
Mean particle size, polydispersity, yield and encapsulation efficiency of the QUEN systems with various weight ratios of QU:EE:PVA

Formulations	Mean particle size (nm)	Polydispersity	Yield (%)	Encapsulation efficiency (%)
QU	4946.0 ± 61.67	1.59 ± 0.28	–	–
QUEN 1:1:1	472.9 ± 107.73[#]	0.74 ± 0.11[#,*]	0.17 ± 0.01	94.8 ± 1.75
QUEN 1:5:5	93.7 ± 8.16[#,*]	0.50 ± 0.10[#,*]	81.9 ± 1.97[*]	99.4 ± 0.02
QUEN 1:10:10	81.9 ± 0.26[#,*]	0.22 ± 0.01[#,*,†]	99.3 ± 0.57[*]	99.9 ± 0.59

All determinations were performed in triplicate and values were expressed as mean ± S.D., $n = 3$.
[#] Significantly different from the QU ($P < 0.001$).
[*] Significantly different compared with the QUEN 1:1:1 ($P < 0.01$).
[†] Significantly different compared with the QUEN 1:5:5 ($P < 0.05$).

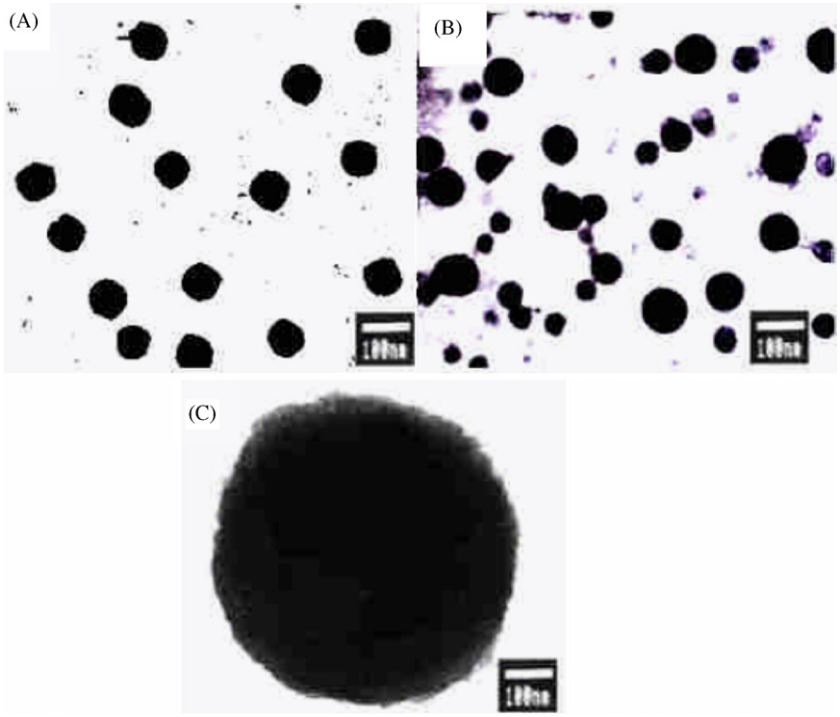

Fig. 2. TEM photographs of the QUEN systems with various weight ratios of QU:EE:PVA. (A) 1:10:10, (B) 1:5:5, (C) 1:1:1.

EE–QU and thus elevated the encapsulation efficiencies of the drug.

3.2. Differential scanning calorimetry

Differential scanning calorimetry curves of the pure components and of the QUEN are displayed in Fig. 3. The endothermic peak of QU was obtained at 326.7 °C corresponding to its melting point. The PVA also showed a broad endothermic peak around at 330 °C. However, no peak melting point was exhibited in the curve of EE and a similar observation has been reported by Jung et al. (1999). In all lyophilized QUEN, we found that the endothermic peak of QU completely disappeared. These results suggested that the drug was dispersed throughout the polymers forming a high-energy amorphous state. Furthermore, the endothermic peaks of all physical mixtures were also absent (data not shown). We suggest that the drug could be fused with the polymers during the heating procedure. Similar findings were also observed by other studies (Tantishaiyakul et al., 1999).

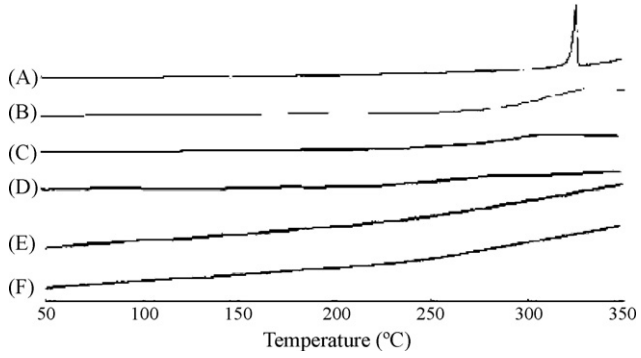

Fig. 3. DSC curves of QU, the carriers, and the QUEN systems with various weight ratios of QU:EE:PVA. (A) QU, (B) PVA, (C) EE, (D) QUEN 1:1:1, (E) QUEN 1:5:5, (F) QUEN 1:10:10.

3.3. Powder X-ray diffraction

The XRD patterns for QU, its physical mixtures, and lyophilized QUEN are shown in Fig. 4. The characteristic peaks of QU exhibited at a diffraction angle of 2θ, 10.73°, 12.33°, 15.87°, 24.41°, 26.50°, and 27.40°, can be inferred to traits of a high crystalline structure. In the case of all physical mixtures,

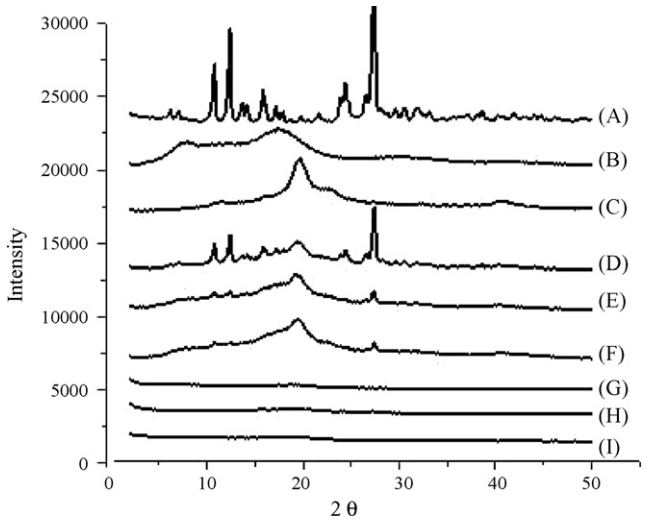

Fig. 4. X-ray diffraction patterns of QU, the carriers, the physical mixtures (PM), and the QUEN systems with various weight ratios of QU:EE:PVA. (A) QU; (B) EE; (C) PVA; (D) PM 1:1:1; (E) PM 1:5:5; (F) PM 1:10:10; (G) QUEN 1:1:1; (H) QUEN 1:5:5; (I) QUEN 1:10:10.

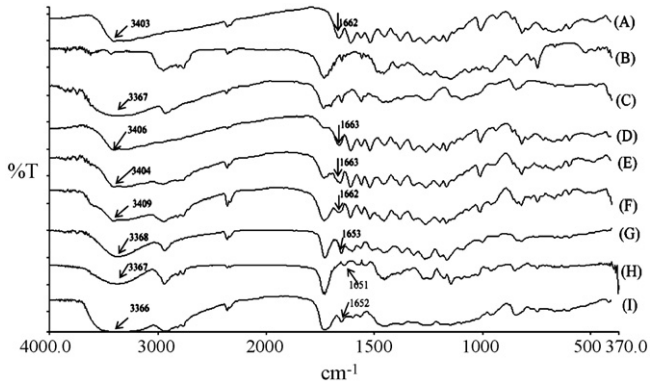

Fig. 5. FT-IR spectra of QU, the carriers, the physical mixtures (PM), and the QUEN systems with various weight ratios of QU:EE:PVA. (A) QU; (B) EE; (C) PVA; (D) PM 1:1:1; (E) PM 1:5:5; (F) PM 1:10:10; (G) QUEN 1:1:1; (H) QUEN 1:5:5; (I) QUEN 1:10:10.

characteristic peaks of QU diminished with an increase in mixing ratios of PVA and EE, however, the crystalline structure of the drug still persisted. Moreover, there were no characteristic peaks appearing on the patterns of all lyophilized QUEN. One explanation for this is that the molecule of QU has been encapsulated or dispersed into EE-PVA polymers when undergoing the nanoprecipitation technique, thus forming an amorphous complex with intermolecular interaction occurring within the matrix. A similar phenomenon has been observed for oridonin dispersed in poly(D,L-lactic acid) (PLA) in which the XRD pattern of oridonin-loaded PLA nanoparticles showed that the drug was in its amorphous state (Xing et al., 2007). Our findings were also in accordance with the above results from the DSC analysis, providing evidence that the crystal structure of QU was indeed converted to an amorphous state.

3.4. Fourier transform infrared

The intermolecular interaction of nanoparticles system was established by FT-IR. Fig. 5 shows QU presenting the characteristic intensities of C=O absorption band at 1662 cm^{-1} and the OH stretch at 3403 cm^{-1}. The spectra of all physical mixtures seemed to be only a summation of QU, PVA, and EE spectra. This observation indicated that no intermolecular interaction occurred in the physical mixtures. However, the spectra from the QUEN showed that the C=O absorption band of QU was shifted toward lower wavenumber and the OH stretch of QU completely disappeared. These results suggested that intermolecular hydrogen bonding occurred in the QUEN and might be stronger than in the physical mixtures. Furthermore, this also indicated that the formation of hydrogen bonding in the QUEN system correlated with the crystalline conversion of QU, and there are several studies that have demonstrated that hydrogen bonding can affect the transformation of drug crystal (Tantishaiyakul et al., 1996, 1999).

3.5. ^{1}H NMR spectroscopic analysis

In ^{1}H NMR analysis, the formation of hydrogen bonding can be also accounted by the change in chemical shifts

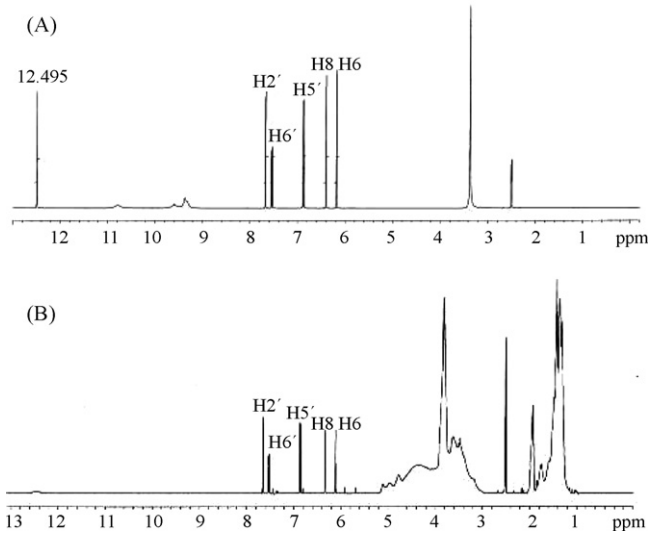

Fig. 6. ^{1}H NMR spectra of QU (A) and the QUEN 1:10:10 (B).

($\Delta\delta = \delta_{complex} - \delta_{pure}$) (Yamamura et al., 2000; Horisawa et al., 2000). The comparative presentation of pure QU and of the QUEN is shown in Fig. 6. The spectrum of QU showed protons on aromatic groups ranging from 6 to 8 ppm, and a strong intramolecular hydrogen bonding at 12.49 ppm, which is a typical shift for intramolecular six-membered ring hydrogen bonding of the C5–OH and C4=O moiety (Exarchou et al., 2002). In the case of the QUEN, the result indicated that the aromatic protons (H6 and H8) of QU were obviously shifted to upfield and the intramolecular hydrogen bonding disappeared. As Table 2 shows, the QU:PVA:EE of 1:10:10 might possess stronger hydrogen bonding than other formulations because its H6 and H8 on the aromatic ring of QU were shifted to about 0.1 ppm. Along with the above findings, these data further demonstrated that the A-ring of QU formed intermolecular hydrogen bonding with the PVA–EE carriers.

3.6. Release rate of quercetin

The dissolution profiles of QU, its physical mixtures, and of the different ratios of QUEN in simulated gastric medium are shown in Fig. 7. The dissolution of pure QU was less than 1%, and the highest ratio of QU:PVA:EE (1:10:10) of the physical mixture dissolved only 8% within 120 min. However, the dissolution profiles of the drug from the QUEN showed faster dissolution than those from the QU and its physical mixtures. Particularly, the drug-release of QU:PVA:EE (1:10:10) of the QUEN was more than 95% within 20 min. In addition, the release rates of QU, its physical mixtures, and of the QUEN conformed to the Higuchi equation and correlation coefficient that ranged from 0.97 to 0.99, as shown in Table 3. The release rates of QU from the physical mixtures and from the QUEN were strongly dependent on the proportion of PVA and EE. Specifically, the release rate of the drug from the QUEN of QU:PVA:EE (1:10:10) was increased 74-fold as compared with pure drug.

Table 2
^{1}H chemical shifts (400 MHz) for QU and the QUEN systems with various weight ratios of QU:EE:PVA

Position	δ (ppm) quercetin	m, J (Hz)	$\Delta\delta$ (ppm)[a]		
			QUEN 1:1:1	QUEN 1:5:5	QUEN 1:10:10
H6	6.183	d, 2.0	−0.020	−0.067	−0.092
H8	6.404	d, 2.0	−0.021	−0.073	−0.099
H5′	6.880	d, 8.4	−0.006	−0.022	−0.031
H6′	7.536	dd, 2, 2.4	−0.003	−0.006	−0.014
H2′	7.674	d, 2.4	−0.010	−0.021	−0.035

[a] $\Delta\delta = \delta_{(QUEN)} - \delta_{(QU)}$.

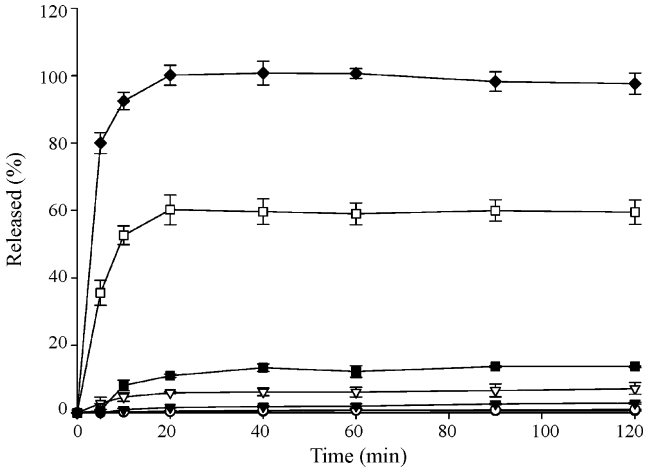

Fig. 7. Dissolution profiles of QU, the physical mixtures (PM), and the QUEN systems with various weight ratios of QU:EE:PVA. Quercetin (●), PM 1:1:1 (◯), PM 1:5:5 (▼), PM 1:10:10 (▽), QEN 1:1:1 (■), QUEN 1:5:5 (□), and QUEN 1:10:10(◆). Values were expressed as mean ± S.D., $n = 6$.

3.7. Antioxidant activity

The QU from the QUEN has been improved in its physicochemical properties especially in that observed for QU:PVA:EE at 1:10:10. Thus, we chose this formulation to assay its antioxidant activity and compared with pure QU dissolved in DMSO (QU–DMSO, positive control) or distilled water (QU–DW).

3.7.1. The DPPH free radical-scavenging assay

The free radical-scavenging effect of QU is attributed to its hydrogen-donating ability. Because the phenolic hydroxyl group of QU molecule could donate the hydrogen to stabilize the free radical and prevent the oxidation of lipid, protein, and DNA, it could therefore further reduce the injuries caused by oxidative stress (Heim et al., 2002). The results on the free radical-scavenging ability of the QUEN, QU–DMSO, and QU–DW are shown in Fig. 8A. The SC_{50} values of QUEN and QU–DMSO were 4.24 ± 0.48 and 7.04 ± 0.85 μg/ml, indicating excellent DDPH radical scavenger activity. The SC_{50} value of QU–DW on the other hand was considerably higher (3746.99 ± 611.68 μg/ml) when compared with QUEN and QU–DMSO ($P < 0.001$). QUEN significantly increased 883-fold on DPPH radical scavenging. The observed radical-scavenging effect of QU from the QUEN at very low concentration suggested that it could be promising against DPPH radicals.

Table 3
Release rate constants (K) of QU, the physical mixtures (PM), and the QUEN systems with various weight ratios of QU:EE:PVA in the simulated gastric fluid

Formulations	Higuchi equation	Correlation coefficient, r	K ($min^{-1/2}$)
QU	$y = 0.1196x - 0.1999$	0.9970	0.120
PM 1:1:1	$y = 0.2087x - 0.4128$	0.9652	0.209
PM 1:5:5	$y = 0.6543x - 1.3104$	0.9724	0.654
PM 1:10:10	$y = 1.3735x - 0.0441$	0.9785	1.374
QUEN 1:1:1	$y = 3.343x - 3.5154$	0.9704	3.343
QUEN 1:5:5	$y = 6.9106x + 28.694$	0.9856	6.911
QUEN 1:10:10	$y = 8.9003x + 60.794$	0.9956	8.900

3.7.2. Anti-superoxide formation and superoxide anion-scavenging activity assay

In xanthine–xanthine oxidase system, xanthine oxidase converts hypoxanthine to xanthine and finally metabolizes it to uric acid. Superoxide anion and hydrogen peroxide are generated in the reaction, and superoxide anion can directly reduce ferri-cytochrome c to ferro-cytochrome c (Gohil et al., 2000). Fig. 8B shows the IC_{50} values of the QUEN and QU–DMSO on anti-superoxide formation, and they were 5.31 ± 0.12 and 5.59 ± 0.15 μg/ml, respectively. QUEN was 493-fold more active than QU–DW (2620.88 ± 107.67 μg/ml) ($P < 0.001$). Moreover, the result of Fig. 8C also shows that the SC_{50} values of the QUEN and QU–DMSO on superoxide anion-scavenging activity were 1.59 ± 0.6 and 1.89 ± 0.11 μg/ml, respectively, and the QUEN was 1377-fold stronger than QU–DW (2189.94 ± 40.31 μg/ml) ($P < 0.001$). These findings demonstrated that the QUEN and QU–DMSO not only possessed strong anti-superoxide formation but also scavenged the superoxide anion. In contrast, the QU–DW was observed to exhibit weak activity when compared with QUEN and QU–DMSO.

3.7.3. Anti-lipid peroxidation assay

Overproduction of free radicals causes a chain reaction of peroxidation on the cell membrane lipid that could lead to cell and tissue death. The inhibitory effect on ferrous ion–vitamin C system-induced lipid peroxidation in rat liver homogenate was used to assess the anti-lipid peroxidation activity of the different QU systems. The anti-lipid peroxidation activity of each sample is shown in Fig. 8D. The IC_{50} value of QUEN and QU–DMSO were 77.17 ± 9.98 and 62.72 ± 7.68 μg/ml, respectively, which indicated that the anti-lipid peroxidation of QUEN

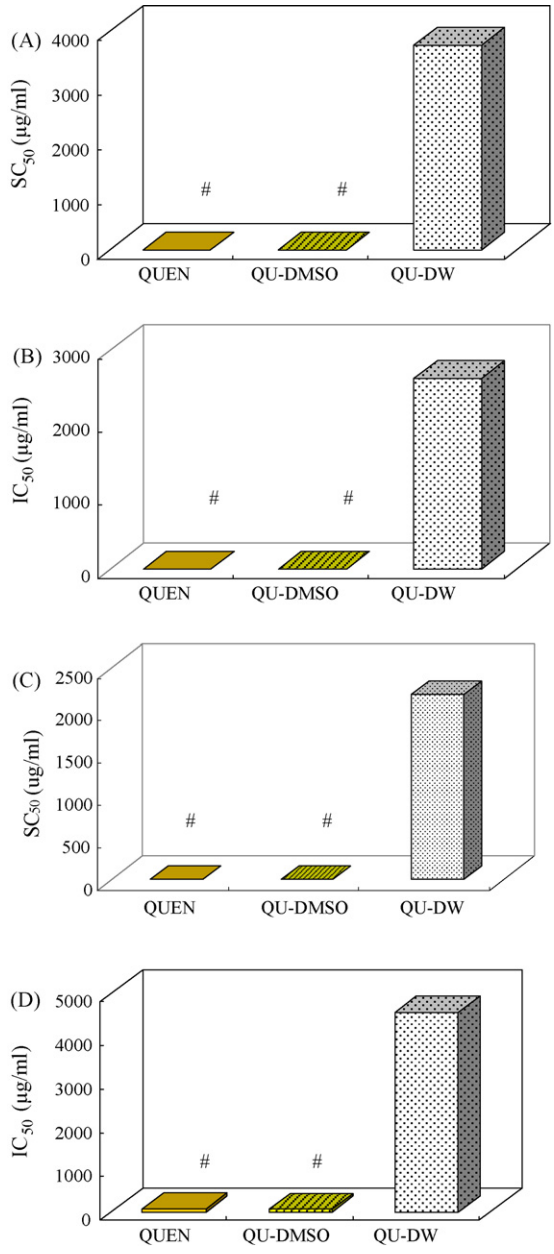

Fig. 8. The antioxidant activities of QUEN, QU–DMSO, and QU–DW in different studies: (A) DPPH radical-scavenging activity; (B) anti-superoxide anion formation; (C) superoxide anion-scavenging effect; (D) anti-lipid peroxidation. All determinations were performed in triplicate and values were expressed as mean ± S.D., $n = 5$. #Significantly different from the QU–DW ($P < 0.001$).

was 59-fold greater than QU–DW (4575.72 ± 525.46 μg/ml) ($P < 0.001$). Previous studies have also demonstrated that the nanoparticles systems of idebenone (Palumbo et al., 2002) and melatonin (Schaffazick et al., 2005) have improved antioxidant and anti-lipid peroxidation activity *in vitro*.

4. Conclusion

The present study demonstrated that the quercetin nanoparticles system (QUEN) was successfully developed by a nanoprecipitation technique. Our studies also established that the release mechanisms of QU from the QUEN were attributed to the reduction of drug particle size, the formation of high-energy amorphous state, and the intermolecular hydrogen bonding. Additionally, the increases of antioxidant activities of QU from the QUEN were correlated with the improvements in physicochemical characterization and dissolution property. Thus, we suggest that the QUEN may be applied in clinical setting and warrant further studies.

Acknowledgements

The authors would like to thank Dr. Horng-Huey Ko (Faculty of Fragrance and Cosmetics, College of Pharmacy, Kaohsiung Medical University) for assistance with ^{1}H NMR analysis and Mrs. Shui-Chin Lu (Department of Mecical Research, Kaohsiung Medical University) for technical support with the TEM.

References

Ader, P., Wessmann, A., Wolffram, S., 2000. Bioavailability and metabolism of the flavonol quercetin in the pig. Free Radic. Biol. Med. 28, 1056–1067.

Bao, J., Cai, Y., Sun, M., Wang, G., Corke, H., 2005. Anthocyanins, flavonols, and free radical scavenging activity of Chinese bayberry (*Myrica rubra*) extracts and their color properties and stability. J. Agric. Food Chem. 53, 2327–2332.

Bala, I., Bhardwaj, V., Hariharan, S., Kharade, S.V., Roy, N., Ravi Kumar, M.N., 2006. Sustained release nanoparticulate formulation containing antioxidant-ellagic acid as potential prophylaxis system for oral administration. J. Drug Target. 14, 27–34.

Bilati, U., Allemann, E., Doelker, E., 2005. Development of a nanoprecipitation method intended for the entrapment of hydrophilic drugs into nanoparticles. Eur. J. Pharm. Sci. 24, 67–75.

Bokov, A., Chaudhuri, A., Richardson, A., 2004. The role of oxidative damage and stress in aging. Mech. Ageing Dev. 125, 811–826.

Castro, I.A., Rogero, M.M., Junqueira, R.M., Carrapeiro, M.M., 2006. Free radical scavenger and antioxidant capacity correlation of alpha-tocopherol and Trolox measured by three in vitro methodologies. Int. J. Food Sci. Nutr. 57, 75–82.

Chang, W.S., Chang, Y.H., Lu, F.J., Chiang, H.C., 1994. Inhibitory effects of phenolics on xanthine oxidase. Anticancer Res. 14, 501–506.

Comalada, M., Camuesco, D., Sierra, S., Ballester, I., Xaus, J., Galvez, J., Zarzuelo, A., 2005. In vivo quercitrin anti-inflammatory effect involves release of quercetin, which inhibits inflammation through down-regulation of the NF-kappaB pathway. Eur. J. Immunol. 35, 584–592.

Dai, J., Nagai, T., Wang, X., Zhang, T., Meng, M., Zhang, Q., 2004. pH-sensitive nanoparticles for improving the oral bioavailability of cyclosporine A. Int. J. Pharm. 280, 229–240.

Exarchou, V., Nenadis, N., Tsimidou, M., Gerothanassis, I.P., Troganis, A., Boskou, D., 2002. Antioxidant activities and phenolic composition of extracts from Greek oregano, Greek sage, and summer savory. J. Agric. Food Chem. 50, 5294–5299.

Fairfield, K.M., Fletcher, R.H., 2002. Vitamins for chronic disease prevention in adults: scientific review. JAMA 287, 3116–3126.

Frijlink, H.W., Eissens, A.C., Hefting, N.R., Poelstra, K., Lerk, C.F., Meijer, D.K., 1991. The effect of parenterally administered cyclodextrins on cholesterol levels in the rat. Pharm. Res. 8, 9–16.

Galindo-Rodriguez, S., Allemann, E., Fessi, H., Doelker, E., 2004. Physicochemical parameters associated with nanoparticle formation in the salting-out, emulsification–diffusion, and nanoprecipitation methods. Pharm. Res. 21, 1428–1439.

Giordano, F.J., 2005. Oxygen, oxidative stress, hypoxia, and heart failure. J. Clin. Invest. 115, 500–508.

Gohil, K., Moy, R.K., Farzin, S., Maguire, J.J., Packer, L., 2000. mRNA expression profile of a human cancer cell line in response to Ginkgo biloba extract:

induction of antioxidant response and the Golgi system. Free Radic. Res. 33, 831–849.

Heim, K.E., Tagliaferro, A.R., Bobilya, D.J., 2002. Flavonoid antioxidants: chemistry, metabolism and structure–activity relationships. J. Nutr. Biochem. 13, 572–584.

Hertog, M.G.L., Hollman, P.C.H., Venema, D.P., 1992. Optimization of a quantitative HPLC determination of potentially anticarcinogenic flavonoids in vegetables and fruits. J. Agric. Food Chem. 40, 1591–1598.

Horisawa, E., Danjo, K., Haruna, M., 2000. Physical properties of solid dispersion of a nonsteroidal anti-inflammatory drug (M-5011) with Eudragit® E. Drug Dev. Ind. Pharm. 26, 1271–1278.

Hsu, C.H., Cui, Z., Mumper, R.J., Jay, M., 2003. Preparation and characterization of novel coenzyme Q10 nanoparticles engineered from microemulsion precursors. AAPS Pharm. Sci. Technol. 4, E32.

Inal, M.E., Kahraman, A., 2000. The protective effect of flavonol quercetin against ultraviolet A induced oxidative stress in rats. Toxicology 154, 21–29.

Jaeschke, H., 2000. Reactive oxygen and mechanisms of inflammatory liver injury. J. Gastroenterol. Hepatol. 15, 718–724.

Jung, J.Y., Yoo, S.D., Lee, S.H., Kim, K.H., Yoon, D.S., Lee, K.H., 1999. Enhanced solubility and dissolution rate of itraconazole by a solid dispersion technique. Int. J. Pharm. 187, 209–218.

Kanadaswami, C., Lee, L.T., Lee, P.P., Hwang, J.J., Ke, F.C., Huang, Y.T., Lee, M.T., 2005. The antitumor activities of flavonoids. In Vivo 19, 895–909.

Kerem, Z., Bravdo, B.A., Shoseyov, O., Tugendhaft, Y., 2004. Rapid liquid chromatography–ultraviolet determination of organic acids and phenolic compounds in red wine and must. J. Chromatogr. A 1052, 211–215.

Klaunig, J.E., Kamendulis, L.M., 2004. The role of oxidative stress in carcinogenesis. Annu. Rev. Pharmacol. Toxicol. 44, 239–267.

Lee, E.S., Lee, H.E., Shin, J.Y., Yoon, S., Moon, J.O., 2003. The flavonoid quercetin inhibits dimethylnitrosamine-induced liver damage in rats. J. Pharm. Pharmacol. 55, 1169–1174.

Liao, K., Yin, M., 2000. Individual and combined antioxidant effects of seven phenolic agents in human erythrocyte membrane ghosts and phosphatidylcholine liposome systems: importance of the partition coefficient. J. Agric. Food Chem. 48, 2266–2270.

McCord, J.M., Fridovich, I., 1969. Superoxide dismutase. An enzymic function for erythrocuprein (hemocuprein). J. Biol. Chem. 244, 6049–6055.

Mu, X., Zhong, Z., 2006. Preparation and properties of poly(vinyl alcohol)-stabilized liposomes. Int. J. Pharm. 318, 55–61.

Mulholland, P.J., Ferry, D.R., Anderson, D., Hussain, S.A., Young, A.M., Cook, J.E., Hodgkin, E., Seymour, L.W., Kerr, D.J., 2001. Pre-clinical and clinical study of QC12, a water-soluble, pro-drug of quercetin. Ann. Oncol. 12, 245–248.

Ohkawa, H., Ohishi, N., Yagi, K., 1979. Assay for lipid peroxides in animal tissues by thiobarbituric acid reaction. Anal. Biochem. 95, 351–358.

Palumbo, M., Russo, A., Cardile, V., Renis, M., Paolino, D., Puglisi, G., Fresta, M., 2002. Improved antioxidant effect of idebenone-loaded polyethyl-2-cyanoacrylate nanocapsules tested on human fibroblasts. Pharm. Res. 19, 71–78.

Peluso, M.R., 2006. Flavonoids attenuate cardiovascular disease, inhibit phosphodiesterase, and modulate lipid homeostasis in adipose tissue and liver. Exp. Biol. Med. 231, 1287–1299.

Pralhad, T., Rajendrakumar, K., 2004. Study of freeze-dried quercetin–cyclodextrin binary systems by DSC, FT-IR, X-ray diffraction and SEM analysis. J. Pharm. Biomed. Anal. 34, 333–339.

Rolo, A.P., Palmeira, C.M., 2006. Diabetes and mitochondrial function: role of hyperglycemia and oxidative stress. Toxicol. Appl. Pharmacol. 212, 167–178.

Sahoo, S.K., Panyam, J., Prabha, S., Labhasetwar, V., 2002. Residual polyvinyl alcohol associated with poly(D,L-lactide-co-glycolide) nanoparticles affects their physical properties and cellular uptake. J. Control. Release 82, 105–114.

Schaffazick, S.R., Pohlmann, A.R., de Cordova, C.A., Creczynski-Pasa, T.B., Guterres, S.S., 2005. Protective properties of melatonin-loaded nanoparticles against lipid peroxidation. Int. J. Pharm. 289, 209–213.

Sehra, S., Dhake, A.S., 2005. Formulation and evaluation of sustained release microspheres of poly-lactide-co-glycolide containing tamoxifen citrate. J. Microencaps. 22, 521–528.

Tantishaiyakul, V., Kaewnopparat, N., Ingkatawornwong, S., 1999. Properties of solid dispersions of piroxicam in polyvinylpyrrolidone. Int. J. Pharm. 181, 143–151.

Tantishaiyakul, V., Kaewnopparat, N., Ingkatawornwong, S., 1996. Properties of solid dispersions of piroxicam in polyvinylpyrrolidone K-30. Int. J. Pharm. 143, 59–66.

Ubrich, N., Schmidt, C., Bodmeier, R., Hoffman, M., Maincent, P., 2005. Oral evaluation in rabbits of cyclosporin-loaded Eudragit® RS or RL nanoparticles. Int. J. Pharm. 288, 169–175.

Venkateswarlu, V., Manjunath, K., 2004. Preparation, characterization and in vitro release kinetics of clozapine solid lipid nanoparticles. J. Control. Release 95, 627–638.

Watson, D.G., Oliveira, E.J., 1999. Solid-phase extraction and gas chromatography–mass spectrometry determination of kaempferol and quercetin in human urine after consumption of *Ginkgo biloba* tablets. J. Chromatogr. B 723, 203–210.

Windrum, P., Morris, T.C., Drake, M.B., Niederwieser, D., Ruutu, T., 2005. Variation in dimethyl sulfoxide use in stem cell transplantation: a survey of EBMT centres. Bone Marrow Transplant. 36, 601–603.

Wong, S.H., Knight, J.A., Hopfer, S.M., Zaharia, O., Leach, C.N., Sunderman, F.W., 1987. Lipoperoxides in plasma as measured by liquid-chromatographic separation of malondialdehyde–thiobarbituric acid adduct. Clin. Chem. 33, 214–220.

Xing, J., Zhang, D., Tan, T., 2007. Studies on the oridonin-loaded poly(D,L-lactic acid) nanoparticles in vitro and in vivo. Int. J. Biol. Macromol. 40, 153–158.

Yamamura, S., Gotoh, H., Sakamoto, Y., Momose, Y., 2000. Physicochemical properties of amorphous precipitates of cimetidine–indomethacin binary system. Eur. J. Pharm. Biopharm. 49, 259–265.

Yu, J.W., Yoon, S.S., Yang, R., 2001. Iron chlorin e_6 scavenges hydroxyl radical and protects human endothelial cells against hydrogen peroxide toxicity. Biol. Pharm. Bull. 24, 1053–1059.

Yuan, Z.P., Chen, L.J., Fan, L.Y., Tang, M.H., Yang, G.L., Yang, H.S., Du, X.B., Wang, G.Q., Yao, W.X., Zhao, Q.M., Ye, B., Wang, R., Diao, P., Zhang, W., Wu, H.B., Zhao, X., Wei, Y.Q., 2006. Liposomal quercetin efficiently suppresses growth of solid tumors in murine models. Clin. Cancer. Res. 12, 3193–3199.

Zili, Z., Sfar, S., Fessi, H., 2005. Preparation and characterization of poly-epsilon-caprolactone nanoparticles containing griseofulvin. Int. J. Pharm. 294, 261–267.